Korean J. Chem. Eng., 39(9), 2548-2554 (2022)
DOI: 10.1007/s11814-022-1103-6

pISSN: 0256-1115
eISSN: 1975-7220

Ultra-thin polymer-encapsulation of $SrAl_2O_4 : Eu^{2+}, Dy^{3+}$ phosphor for enhanced hydrolytic resistance

Hyang Moo Lee*,‡, Jun Hee Heo*,‡, Jin Chul Kim**,†, Jin Joo*,†, and In Woo Cheong*,***,†**

*Department of Applied Chemistry, Kyungpook National University, Daehak-ro 80, Buk-gu, Daegu 41566, Korea
**Department of Specialty Chemicals, Division of Specialty and Bio-based Chemicals Technology, Korea Research Institute of Chemical Technology (KRICT), Ulsan 44412, Korea
***Department of Hydrogen & Renewable Energy, Kyungpook National University, Daehak-ro 80, Buk-gu, Daegu 41566, Korea
(*Received 21 December 2021 • Revised 2 March 2022 • Accepted 9 March 2022*)

Abstract−Eu^{2+} and Dy^{3+} doped strontium aluminates ($SrAl_2O_4 : Eu^{2+}, Dy^{3+}$) are well known green light emitting materials with a long-lasting afterglow property; however, $SrAl_2O_4 : Eu^{2+}, Dy^{3+}$ is readily hydrolized under ambient moisture conditions, which impedes industrial applications. In this work, $SrAl_2O_4 : Eu^{2+}, Dy^{3+}$ phosphor was encapsulated by layer-by-layer (LbL) and coacervation methods for the formation of ultra-thin polymeric capsulation layer. Morphology of the phosphor and polymer-encapsulated phosphors was characterized by scanning electron microscopy (SEM). The amount and thickness of the encapsulated polymer layers were analyzed by thermogravimetric analysis (TGA) and atomic force microscopy (AFM), and the polymer content for the phosphor encapsulated by LbL was estimated to be 0.08 wt% with a shell thickness of 11 nm. After pristine phosphor and encapsulated phosphor samples were immersed in water for 24 h, the photoluminescence (PL) intensity was measured to compare the water-resistant performance. The polymer-encapsulated phosphors by LbL and coacervation methods were maintained for 85.7 and 93.5% of pristine phosphors, respectively, while PL intensity of the pristine phosphor was observed as 18.1% after immersion in water for 24 h. The change in pH was monitored under the same conditions. The pH for the dispersion of polymer-encapsulated phosphors by LbL and coacervation methods was measured as 10.27 and 9.63, respectively, while pH for the dispersion of the pristine phosphor was observed as 11.99. This research may provide a wider option for the encapsulation methods of particulate materials for applications where encapsulation with very thin layer of polymer is needed, because the encapsulation process inevitably lowers both the content of active ingredients and consequently their performance as well.

Keywords: Phosphor, Encapsulation, Layer-by-Layer, Coacervation, Hydrolytic Resistance

INTRODUCTION

Strontium aluminates doped with Eu^{2+} and Dy^{3+} ($SrAl_2O_4 : Eu^{2+}, Dy^{3+}$) are commercially available phosphors, emitting green light (~510 nm). These phosphors have been widely studied due to their long-lasting afterglow property for longer than ~1,000 minutes [1-3]. However, $SrAl_2O_4 : Eu^{2+}, Dy^{3+}$ phosphors are susceptible to hydrolysis in ambient moisture conditions, a fatal drawback limiting industrial applications such as road signs and safety marks to improve visibility in rainy weather or at night [4-7]. When they are exposed to water molecule, hydrolysis takes place by breaking O-Sr-O bonds to produce aqueous strontium hydroxide and aluminum hydroxide precipitation [8-10].

$$SrAl_2O_4 + 4H_2O \rightarrow Sr^{2+}(aq) + 2OH^-(aq) + 2Al(OH)_3(s) \quad (1)$$

To address the issue of poor water resistance of phosphor, various methods have been developed to form a protective layer on the phosphor surface. The most convenient procedure is to modify the phosphor surface with phosphate [11] or fluoride layers [10]. However, despite the enhanced water resistance of the surface-modified phosphors, the use of toxic phosphoric acid or HF from the thermal decomposition of NH_4F restricts the employment of these procedures for the mass production of phosphors. In addition, it is very difficult to control the reaction rate of the phosphor surface because of the high reactivity of the phosphor surface.

The encapsulation method is another versitle route for improving the hydrolytic resistance of phosphors using organic or inorganic materials [12-16]. There are several ways to encapsulate phosphors, such as multi-core structure including phosphor-embeded bead or matrix systems [5,17,18]. These approaches demonstrated improved stability against water; however, hydrolytic resistance was estimated in a few hour time scale.

Recently, inorganic/organic encapsulation has been reported to obtain a phosphor with high hydrolytic resistance. For example, Shi et al. used several silane coupling agents to make the phosphor surface hydrophobic, yielding enhanced hydrolytic resistance [19]. Yan et al. used silica and poly(methyl methacrylate-*co*-butyl acry-

†To whom correspondence should be addressed.
E-mail: jckim81@krict.re.kr, joojin@knu.ac.kr, inwoo@knu.ac.kr
‡These authors contributed equally on this work.

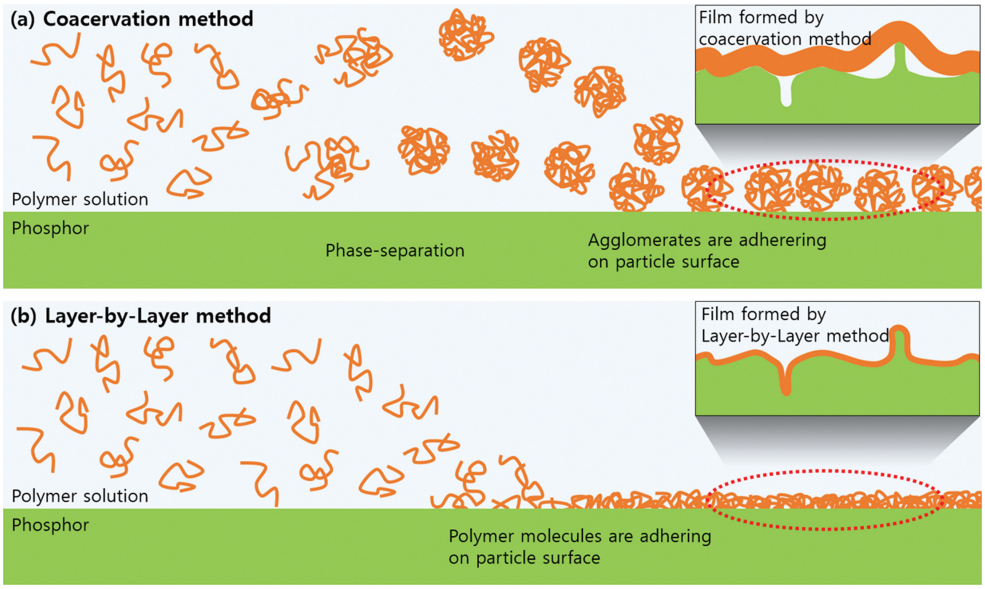

Fig. 1. Schematic description of the encapsulation mechanism by (a) coacervation and (b) LbL methods. In coacervation, PGMA was used and then crosslinked with TEPA. In the case of LbL, PGMA and PEI were used alternately, but this was omitted in this figure.

late) bilayers to coat phosphors by heterogeneous precipitation and *in situ* emulsion polymerization, respectively, and the encapsulated phosphors were used for waterborne UV acrylic coatings [20]. Lei et al. also obtained a phosphor with improved hydrolysis resistance by 71.7% by using a double-layer coating of silica and poly(acrylic acid-*co*-methyl methacrylate) to improve the hydrolysis resistance of the phosphor [21].

In most approaches using inorganic or organic encapsulation layers, the inorganic layer is difficult to completely cover the phosphor surface, and a polymer coating that is too thick to scatter or absorb emitted and luminance light, reducing quantum efficiency. In addition, since the encapsulation process introduces a layer to protect the active ingredient, the content and performance of the active ingredient are often reduced. Therefore, it is necessary to introduce an ultra-thin polymer coating on the phosphor to provide high loading content and high hydrolysis resistance.

In the present work, $SrAl_2O_4:Eu^{2+}, Dy^{3+}$ phosphors were encapsulated with two different methods (Fig. 1). For the shell material, an acrylic polymer with epoxy functionality was prepared by free-radical polymerization. An encasupated phosphor with ultra-thin polymer layer was prepared by layer-by-layer (LbL), and a phosphor which had a relatively thick polymer layer was prepared by coacervation. Then, the morphologies and hydrolytic resistant properties of the encapsulated phosphors were studied with pH variations and the intensity changes of emitted light over time after the phosphors were placed in water.

EXPERIMENTAL

1. Materials

Methyl methacrylate (MMA, 99.0%, Daejung), glycidyl methacrylate (GMA, 97.0%, Merck), butyl acrylate (BA, 99.5%, Junsei), polyethyleneimine (PEI, molecular weight=10 kg/mol, 99%, Alfa Aesar), 1,4-dioxane (99.5%, Daejung), *N,N*-dimethyl formamide (DMF, 99.5%, Duksan), acetone (99.5%, Duksan), hexane (95%, Duksan), tetradecane (99.0%, Wako), (3-aminopropyl)triethoxysilane (APTES, 99%, Merck), ethanol (99%, Duksan), and tetraethylenepentamine (TEPA, 95%, TCI) were used as received. 2,2′-Azobis (2-methylpropionitrile) (AIBN, 98%, Junsei) was used after recrystallization in methanol. Toluene (95%, Duksan) was distilled from sodium benzophenone ketyl under nitrogen atmosphere to remove moisture. $SrAl_2O_4:Eu^{2+}, Dy^{3+}$ phosphor (PL70) was kindly donated by Ukseung Chemical, Korea. *N,N*-dimethyl formamide (DMF, HPLC grade, Daejung) was used for the eluent of size exclusive chromatography with 0.01 M of litium bromide (LiBr, HPLC grade, Merck).

2. Synthesis of Poly(methyl methacrylate-*ran*-*n*-butyl acrylate-*ran*-glycidyl methacrylate) (PGMA)

PGMA copolymer was prepared by free-radical copolymerization with three different monomers of MMA, BA, and GMA. For the reaction, MMA, BA, GMA, and AIBN were dissolved in 1,4-dioxane with the molar ratios of 43.4, 46.6, 10, and 1 molar ratios, respectively. The sealed reactant mixture was bubbled with N_2 gas for 30 min to remove oxygen in the flask, and the solution teperature was kept at 70 °C for 16 h in a pre-heated oil bath. After the reaction, the resulting mixture was dried in a vacuum oven and the prepared polymer was used without further purification. Finally, the prepared PGMA was dissolved in DMF with 20 wt% concentration for the next step.

3. Surface Modification of Phosphor with APTES

The surface of PL70 was modified with APTES. The reaction was carried out by refluxing a mixture composed of 5 mL of APTES and 10.0 g PL70 in 200 mL of anhydrous toluene for 24 h under N_2 atmosphere. Thereafter, the reaction mixture was filtered and washed several times with toluene and ethanol, and finally dried in a convection oven at 60 °C for 24 h.

4. Encapsulation of Phosphor *via* LbL Technique

Prepared PGMA and PEI were used for the encapsulation of

phosphor via LbL technique to produce ultra-thin and defect-less polymer layer on phosphor. The samples were labeled as *n@P*, where *n* and *P* denote the number of polymer layers and the final material coated on phosphor, respectively. In the PGMA coating step, a desired amount of *0@APTES* and the same weight of 20 wt% PGMA solution were added into the reactor. Then, the whole reaction mixture was rotated at 100 rpm to prevent phosphor particles from agglomeration and the reaction proceeded in a pre-heated oil bath at 120 °C for 1 h. After the reaction, the reaction mixture was washed with pure DMF and acetone, then dried. Finally, the PGMA-coated phosphor (*1@PGMA*) was obtained and used for further encapsulation step.

In the PEI (second polymer layer) coating step, the desired amount of *1@PGMA* and the same weight of 20 wt% PEI solution in DMF were added into the reactor. Then, the whole reaction mixture was rotated at 100 rpm in a pre-heated oil bath at 120 °C for 1 h. After 1 h, the reaction mixture was washed with pure DMF and acetone, then dried. As a result, PEI coated phosphor (*2@PEI*) was obtained. For third or more layer coating steps, the same procedures were repeated using PGMA solution or PEI solution, alternately, and finally, *9@PGMA* sample was obtained.

5. Encapsulation of Phosphor *via* Coacervation Phase Separation Process

As a control sample, coacervation method was also applied to encapsulate phosphors with PGMA. For coacervation, 1 g of APTES-coated phosphor and 1 mL of chloroform was added into reactor with 0.124 mL of 20 wt% PGMA solution in DMF solution and 0.653 mg of TEPA. Then, 5 mL of tetradecane was slowly added for 1 h using a microsyringe pump (KDS LEGATO® 100, KD Scientific, USA) while rotating the reactor. The mixture was then immersed in pre-heated oil bath at 120 °C for 3 h with stirring using an overhead stirrer. After the reaction, the phosphor was washed with acetone and dried under vacuum. Finally, yellowish powder was obtained and labeled as Coac.1000.

6. Characterization

For polymer analyses, nuclear magnetic resonance (NMR, AVANCE III 500, Bruker) in chloroform-*d* with 0.05 wt% tetramethyl silane was used. Molecular weights ($\overline{M}_n$) and dispersity ($Đ_M$) of PGMA were measured using size exclusion chromatography (SEC, NP-4000 GPC system, Futecs) with DMF as eluent (with 0.01 M LiBr). Solvent delivery pump (P-4000, Futecs, Korea), column oven (AT-4000, Futecs, Korea), and RI detector (RI-101, Shodex, Japan) were used for the SEC system with a series of columns (KD-803, 804, 805, Shodex, Japan). PMMA narrow standards (2,890 to 955,000 g/mol, Shodex, Japan) were used for calibration.

To monitor the crosslinking reaction of PGMA during the encapsulation, 20 wt% PEI solution in DMF or desired amount of TEPA was mixed with 20 wt% PGMA solution in DMF, and the mixture was immersed in a pre-heated oil bath at 120 °C for 1 h. After the reaction, the crosslinked organogels were completely dried under vacuum, and used for differential scanning calorimetry (DSC, Q20, TA Instr.), Fourier-transform infrared spectroscopy (FT-IR, IR prestige-21, Shimadzu), and gel content measurements.

For the DSC analysis, the samples were loaded into standard Tzero hermetic pans (aluminum, TA Instr.). The measurements were conducted under N_2 gas flow of 50 mL min^{-1} over a temperature range from −70 °C to 150 °C with a heating rate of 10 °C min^{-1}. FT-IR spectra were collected in attenuated total reflectance (ATR) mode in the wavenumber range of 400 to 4,000 cm^{-1} at room temperature. For the gel content, crosslinked polymers (approx. 0.2 g, W_p) were mixed with 10 mL of DMF. After 24 h, DMF was decanted, and the crosslinked polymers were rinsed with pure DMF and dried under vacuum. The weight of dried polymers (W_{ex}) was measured by microbalance (BM-22, AND). The gel content was determined by W_{ex}/W_p.

Thermogravimetric analysis (TGA, Q500, TA Instr.) was carried out at a temperature range of 25 to 700 °C with a heating rate of 10 °C/min under air flow after maintained at 100 °C for 10 min.

Scanning electron microscope (SEM, 15 kV, 10 mA, SU8220, Hitachi) with energy dispersive X-ray spectroscopy (EDS, 15 kV, Ultim Max 100, Oxford) was used to observe polymer morphology. Before measurement, the samples were coated by platinum sputtering.

The thickness of polymer layer coated by layer-by-layer technique was measured by atomic force microscopy (AFM, XE7, Park Systems) mounted with a non-contact mode cantilever (PPP-NCHR, Park Systems). Since the phosphor surface was too uneven to measure polymer thickness directly, Si wafer was coated by LbL technique to estimate the coating thickness. For this experiment, Si wafer was washed and immersed in anhydrous toluene containing 1 vol% APTES for 30 min at room temperature and then rinsed with ethanol. Then the APTES-coated Si wafer was immersed in DMF solution containing 20 wt% PGMA or PEI alternatively at 120 °C for 1 h. The polymer-coated Si wafer was washed with ethanol after each step. The coated Si wafer surface was scratched using a razor blade and the thickness difference around the scratched edge was measured in AFM.

For the hydrolysis test, a pH meter (UP-10, Denver Instr.) and photoluminescence (PL, RF-5301PC, Shimadzu) spectrofluorometer were used. To hydrolyze the samples, 0.2 g of each sample was immersed in a 50 mL of deionized (DI) water (Elga Labwater, Purelab Option Q7) and kept under undisturbed conditions. The pH of supernatant water was measured with the desired time interval. The PL intensity of the samples before and after immersion in water for 24 h was measured and compared. The samples in the quartz cuvette were irradiated with 50 lumens white LED light for 60 s to fully excite the phosphors and the PL intensity was measured in a wavelength range from 400 to 650 nm for 1 s.

Photographs of samples before and after hydrolysis were also taken by a Samsung Galaxy Note 20 ultra 5G by fixing the parameters of exposure time 50 ms and ISO 1600. To place the sample on the slide glass to the same thickness, five layers of 3 M magic tape (ca. 280 μm) were overlapped as a height guide. For the photos of glowing phosphor, 50 lumens white LED light was irradiated on a sample in a darkroom for 60 s, and then photographed after 10 s.

RESULTS AND DISCUSSION

1. Characterization of PGMA Copolymer

The composition and molecular weights of prepared PGMA copolymer were characterized by ^{1}H NMR and SEC. As shown in

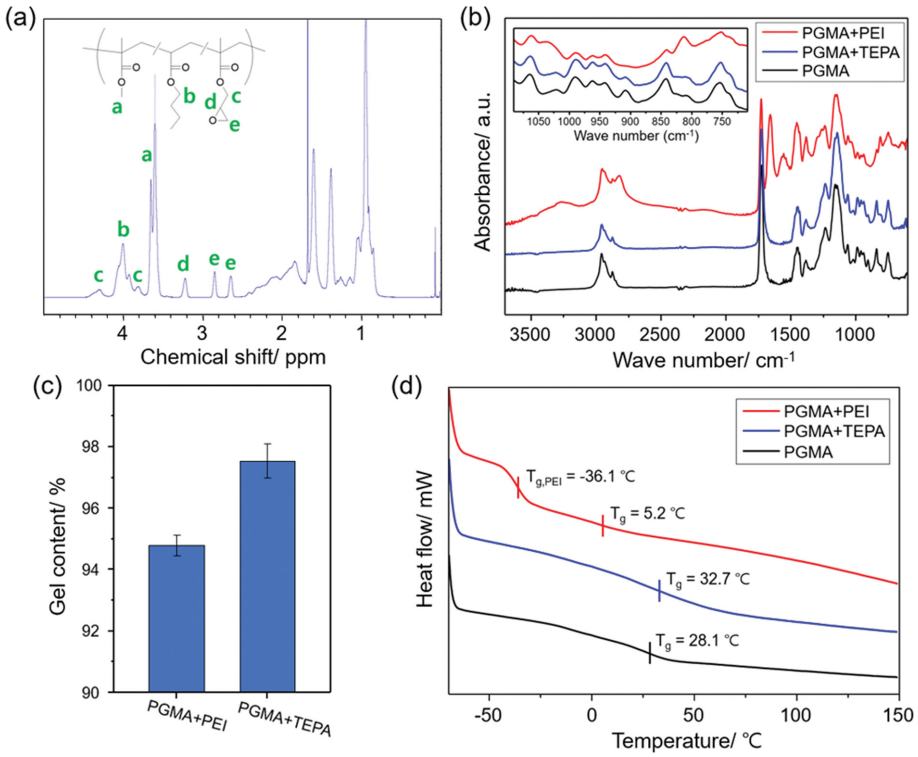

Fig. 2. (a) ^{1}H NMR spectra for PGMA copolymer, (b) FT-IR spectra of PGMA copolymer and crosslinked PGMA copolymers with PEI or TEPA, (c) gel content, and (d) DSC curves of the copolymers.

Fig. 2(a), chemical shifts at 2.64 and 2.84 ppm from methylene of oxirane, at 3.21 ppm from methine of oxirane, and at 3.80 and 4.30 ppm from methylene in GMA unit were observed. The chemical shifts at about 3.6 and 4.0 ppm from -O-CH_3 of MMA and -O-CH_2- of BA were observed, respectively. From the area of these peaks, the composition of each monomer was calculated as 4.34 : 4.66 : 1.0 for MMA, BA, and GMA in molar ratio, respectively. $\overline{M}_n$ and $Đ_M$ of PGMA were measured as 2.67 kg/mol and 2.03, respectively.

The IR spectra of PGMA and crosslinked PGMA samples are shown in Fig. 2(b). The intensity of the spectra was normalized by the intensity of C=O band at 1,728 cm^{-1}. PGMA crosslinked by PEI sample (PGMA+PEI) exhibited N-H band at 3,260 cm^{-1} even after the polymers were crosslinked because PEI has excess amount of amine compared to oxirane moiety; however, N-H band of PGMA crosslinked by TEPA (PGMA+TEPA) was not observed because amine was used in a very small amount. However, disappeared or reduced oxirane band at 908 cm^{-1} for PGMA+PEI and PGMA+TEPA proves the crosslinking reaction has properly progressed, and gel content shown in Fig. 2(c) also proves that the crosslinking reaction in the presence of TEPA or PEI was well done.

Glass transition temperatures (T_gs) of PGMA and crosslinked polymer samples were measured by DSC, as shown in Fig. 2(d). The DSC curves were taken from the second heating cycle. The T_g for PGMA copolymer was measured as 28.1 °C, and the T_g for PGMA+TEPA was measured as 32.7 °C, and which is 4.6 °C higher than the T_g before it was crosslinked. However, PGMA+PEI shows two T_gs as −36.1 and 5.2 °C from used PEI and crosslinked PGMA moiety, respectively. The T_g for crosslinked PGMA was even lower than prepolymer of PGMA because of blended PEI used as a crosslinker.

2. Encapsulation of $SrAl_2O_4 : Eu^{2+}$, Dy^{3+} Phosphor

Surface the morphology of PL70 and polymer-encapsulated phosphors was characterized by SEM. The SEM image in Fig. 3(a) shows a rough surface of pristine phosphor PL70. In the case of Coac.1000, a smooth surface is observed because of the complete coverage of relatively thick polymer layer (Fig. 3(b)). On the other hand, the SEM image of *9@PGMA* still shows a rough surface because the polymer layer is not thick enough to cover the rough surface of the pristine phosphor surface (Fig. 3(c)).

Elemental analysis results taken from EDS reveal the presence of polymer layers, as shown in Fig. 3(d). Aluminum and carbon content of APTES-modified phosphor (*0@APTES*) was estimated to be 19.8 and 16.7 atomic %, and 17.8 and 33.9 atomic % for the 9-layer polymer coated phosphor (*9@PGMA*), respectively. With thicker polymer layers, however, aluminum content (the component of phosphor) decreases while carbon content (the component of polymer) increases. These results strongly support that thin layers of PGMA and PEI polymers were successfully formed on phosphor surface by LbL technique. In the case of Coac.1000, the aluminum and carbon content was measured as 9.27 and 57.53 atomic %, respectively. For the measurement of the exact thickness of polymer coating formed by LbL technique, Si wafer was used instead of phosphor for LbL technique. As shown in Fig. 3(f), 9-layers of coated polymer thickness was about 11.2 nm taken from AFM.

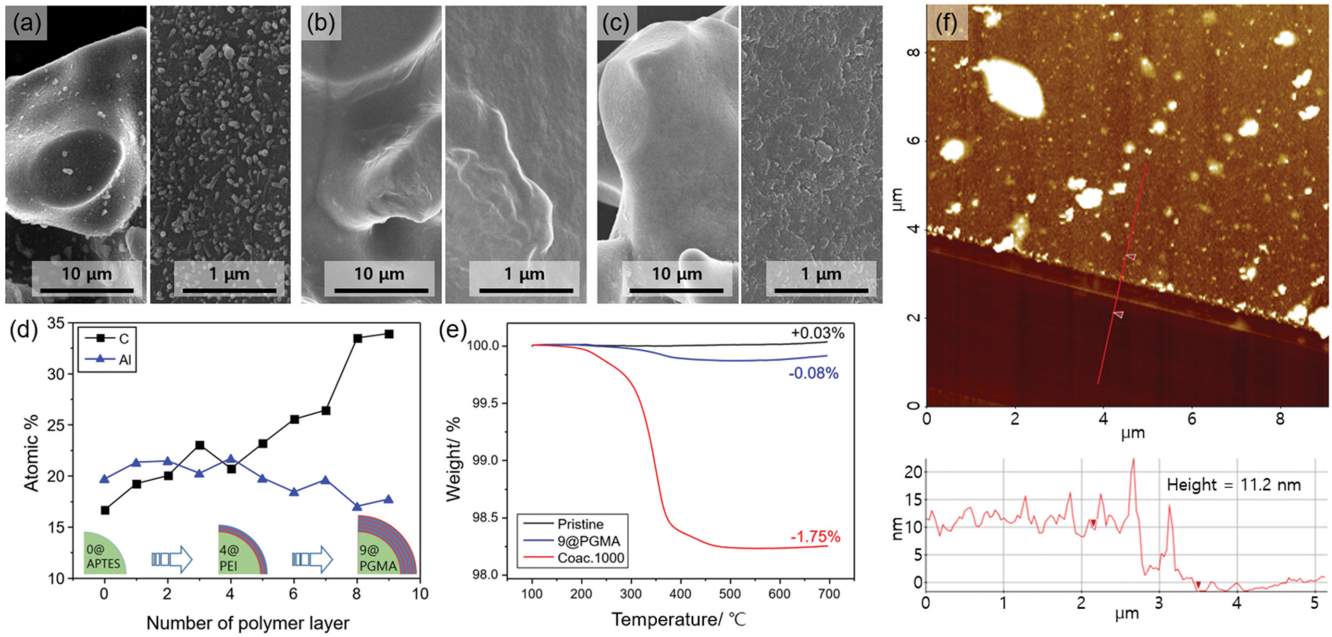

Fig. 3. SEM images of (a) PL70, (b) Coac.1000, and (c) *9@PGMA*, and (d) SEM-EDS results for the encapsulated phosphors by LbL technique, (e) TGA results for pristine $SrAl_2O_4:Eu^{2+}$, Dy^{3+} phosphor and encapsulated samples, and (f) the thickness of 9-layer polymer coatings on Si wafer coated by LbL technique.

TGA analysis of Fig. 3(e) confirmed that the polymer layer was burnt out at over 230 °C. The pristine phosphor shows no weight loss in the experimental temperature range, while the polymer coated samples lose some weight. In more detail, the weight of Coac.1000 decreased by 1.75%, and the weight of *9@PGMA* decreased by 0.08%, which means the amount of polymer incorporated into coating layer for *9@PGMA* was over twenty times smaller compared to that for Coac.1000. The polymer layer thickness can be estimated from TGA results with assuming that PL70 is a spherical particle with a radius of 35 μm, and the polymer density is 1 g/mL. In the case of *9@PGMA*, the polymer thickness was calculated as ca. 33 nm, and for Coac.1000, the polymer thickness was calculated as ca. 712 nm.

3. Hydrolytic Resistance of Polymer-encapsulated $SrAl_2O_4:Eu^{2+}$, Dy^{3+} Phosphor

Pristine PL70 has a fine power form as shown in Fig. 4(a). However, after polymer coating with coacervation, the particles are agglomerated although they are still powdery. On the other hand, the fine powdery phase was retained after polymer-coating by LbL process. After hydrolysis by the immersion of the phosphors in water, no changes in appearance and luminescence intensity were observed for Coac.1000 and *9@PGMA* samples in contrast to pristine PL70 as shown in Fig. 4(b).

The aqueous dispersion containing $SrAl_2O_4:Eu^{2+}$, Dy^{3+} phosphor becomes basic due to the hydrolysis reaction as shown in Eq. (1). From this reaction, hydrolytic stability of the pristine phosphor and polymer-encapsulated phosphor against water was studied. The pH changes of pristine and polymer-encapsulated phosphors by LbL or coacervation methods were monitored over time as shown in Fig. 4(c). As an experimental result, the pH for DI water was 6.80, and this surged right after PL70 was added, finally approaching pH 11.99 in 24 h. In the case of Coac.1000, the pH changed from 6.8 to 9.63 after 24 h immersion. For the *9@PGMA*, the pH changed from 6.8 to 10.27 after 24 h.

PL spectra also show similar results to pH data. Fig. 4(d) shows the PL spectra of pristine PL70, Coac.1000, and *9@PGMA* before and after the immersion of phosphors in water for 24 h. As shown in the PL plots, intense emission light was drastically reduced after the immersion in water. In contrast, almost no noticeable decrease in PL strength was seen in Coac.1000 after polymer coating. Similarly, *9@PGMA* with a much thinner polymer layer on the PL70 exhibited comparable PL strength to Coac.1000 with a thicker polymer layer. After 24 h of hydrolysis, the normalized maximum PL intensity remained at 18.1, 93.5, and 85.7% of the initial emission intensity for PL70, Coac.1000 and *9@PGMA*, respectively (Fig. 4(e)). Note that the polymer layer of *9@PGMA* is much thinner than that of Coac.1000. This indicates that LbL is a very efficient process to overcoat $SrAl_2O_4:Eu^{2+}$, Dy^{3+} phosphor, thereby leading to high hydrolytic resistance.

It is known that the permeation rate of water in a polymer membrane is inversely propertional to the square of the membrane thickness ($L=\frac{l^2}{6D}$ where L is time-lag, l is membrane thickness, and D is diffusion coefficient) [22]. As can be seen from the TGA results in the previous section, the polymer thickness of the sample formed by coacervation was over 20 times thicker than that of the sample formed by LbL, which means the permeation rate for Coac.1000 is about 400 times slower than that for 9@PGMA. However, in the PL study, the difference between the two samples after the hydrolysis test was not significant. These results suggest that the LbL method forms a denser coating layer on the phosphor with lesser deffect compared to coacervation. In this study, the immersion

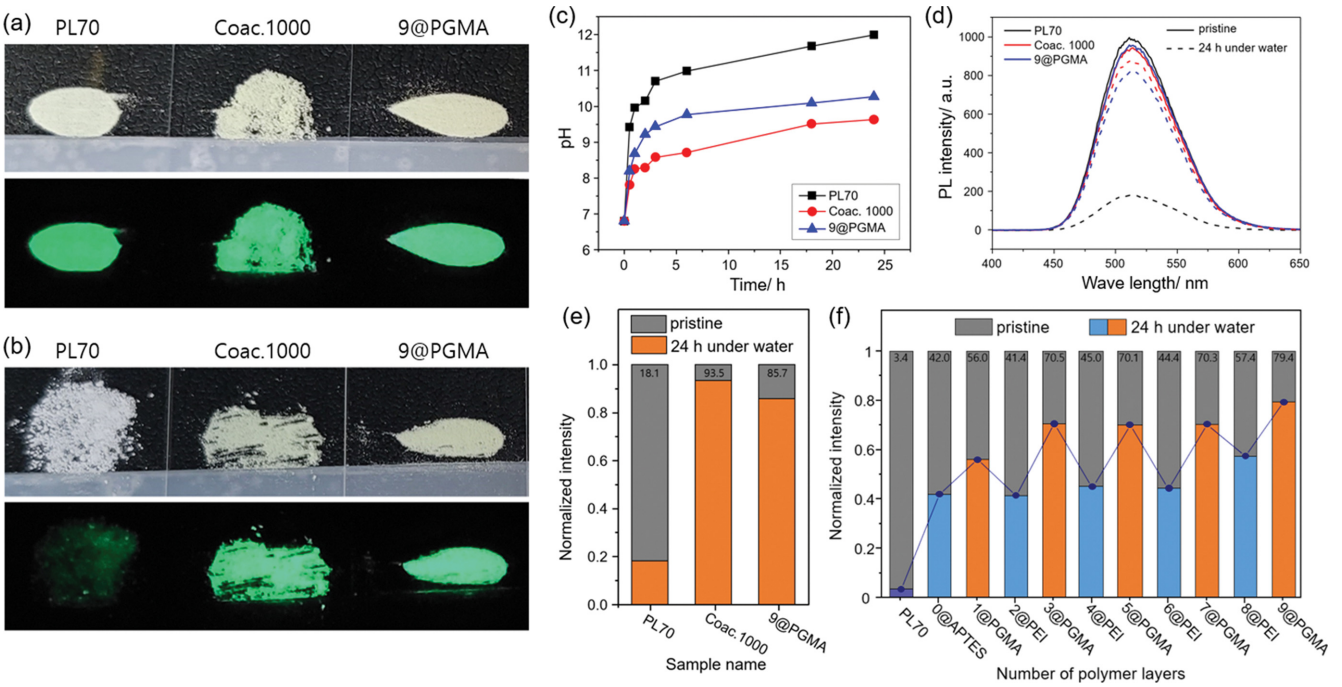

Fig. 4. Photographs of $SrAl_2O_4:Eu^{2+}$, Dy^{3+} pristine phosphor (PL70) and encapsulated phosphors (Coac.1000 and *9@PGMA*) (a) before and (b) after immersion in DI water for 24 h, (c) variation in pH value of water in the presence of pristine or encapsulated phosphors, (d) PL spectra of each sample before and after immersion in water for 24 h, (e) normalized PL intensity of the encapsulated phosphors, and (f) normalized PL intensity for encapsulated phosphors by LbL technique before and after immersion in water for 24 h.

time for PL measurements was designed to be fixed at 24 h, and it was used to observe the water resistance for easy comparison because the degree of corrosion is linearly proportional to time [23, 24], and the corrosion rate is inversely proportional to the square of the coating thickness [22] under the condition that all corrosion conditions and coating quality are the same. Fig. 4(c) shows the hydrolysis tendency for the phosphor up to 24 h by the pH data. Other than time or coating thickness, many other factors may affect to the stability of phosphor in water, such as temperature or pH of environment. Alumina formed by corrosion of phosphor under coating layer also may damage the coating layer to cause acceleration of hydrolysis of the phosphor. However, these factors are not of our interest, so we have not discussed them in the article.

The changes in normalized PL intensities with successive coating of each polymer layer formed by LbL technique also are shown in Fig. 4(f). For these measurements, aqueous phosphor sample dispersions were shaken for every hour to accelerate hydrolysis speed to observe a clear trend in PL decrease. Interestingly, the hydrolytic resistance did not linearly increase with the increase in the number of coated polymer layers. The overall tendency of the hydrolytic resistance increases with the number of polymer layer coatings, but the samples coated PGMA at the last layer (1, 3, 5, 7, and 9 layer coated samples) have relatively higher hydrolytic resistance compared to the samples coated PEI at the last layer (0, 2, 4, 6, and 8 layer coated samples). From the results, we found that the degree of hydrophobicity of shell material plays an important role in hydrolytic resistance; PGMA is the copolymer synthesized from hydrophobic MMA and BA monomers, and APTES and PEI are hydrophilic. When the outmost surface is coated by PGMA, the phosphor surface is more hydrophobic than the surface of PEI coating, which imparts higher hydrolytic resistance.

During the coacervation coating process, poor solvent was added into polymer solution, producing polymer agglomerate in the solution. Then the agglomerate moved to the particle surface and formed a film on the phosphor surface. In the case of LbL technique, on the other hand, the polymer molecules directly moved and attached on the particle surfaces. Thus, the coacervation method produces thick coatings, and it may have voids or defects of a small gap such as cracks because large polymer agglomerates cannot reach into small gaps. However, LbL method produces a very thin, uniform, and defect-free film because polymers in a molecular level fill all the gaps even if they form in nanoscale. Therefore, although the polymer thickness of *9@PGMA* is much thinner compared to Coac.1000, it shows similar hydrolytic resistance to Coac.1000.

CONCLUSION

Acrylic copolymer bearing epoxide (PGMA) was synthesized through free-radical polymerization and used for the encapsulation of $SrAl_2O_4:Eu^{2+}$, Dy^{3+} phosphor. For the encapsulation, two different methods were used for comparison: LbL and coacervation. The coated polymer layers were quantitatively analyzed by SEM-EDS, TGA, and AFM measurements. The phosphor encapsulated by LbL method (*9@PGMA*) showed an ultra-thin polymer coating thickness of about 11 nm with a thin 9-polymer layers, whereas the phosphor encapsulated by coacervation (Coac.1000) showed a much thicker polymer layer compared to *9@PGMA*. Hydrolytic resistance of each sample was studied by the change in

pH and PL intensity. As a result, *9@PGMA*, having extremely thinner polymer coating thickness compared to Coac.1000, exhibited very high hydrolytic resistance comparable to Coac.1000. In the case of coacervation method, large polymer agglomerates adhered to the surface during the encapsulation process, whereas polymer molecules were adhering to the surface in LbL method. Therefore, much thinner and defect-free shell layer on phosphors can be achieved by LbL method. Thus, through LbL method, we can finely control the shell thickness at molecular level. The results of this research are expected to help select the appropriate encapsulation method depending on its purpose.

ACKNOWLEDGEMENT

The authors are very grateful for financial support from the Korea Agency for Infrastructure Technology Advancement (Grant No. 19POQW-B152733-01).

REFERENCES

1. R. E. Rojas-Hernandez, F. Rubio-Marcos, M. A. Rodriguez and J. F. Fernandez, *Renew. Sustain. Energy. Rev.*, **81**, 2759 (2018).
2. H. Yamamoto and T. Matsuzawa, *J. Lumin.*, **72-74**, 287 (1997).
3. P. Zeng, X. Wei, M. Yin and Y. Chen, *J. Lumin.*, **199**, 400 (2018).
4. J. Nance and T. D. Sparks, *Prog. Org. Coat.*, **144**, 105637 (2020).
5. J. I. Park, S. H. Jeong and I. W. Cheong, *J. Adhes. Interface*, **17**, 110 (2016).
6. Y. Bi, J. Pei, Z. Chen, L. Zhang, R. Li and D. Hu, *Int. J. Pavement Res. Technol.*, **14**, 252 (2021).
7. J. Nance and T. D. Sparks, *Prog. Org. Coat.*, **148**, 105749 (2020).
8. X. Lu, *Mater. Chem. Phys.*, **93**, 526 (2005).
9. Y. Zhu, M. Zheng, J. Zeng, Y. Xiao and Y. Liu, *Mater. Chem. Phys.*, **113**, 721 (2009).
10. H. N. Luitel, T. Watari, T. Torikai, M. Yada, R. Chand, C.-N. Xu and K. Nanoka, *Appl. Surf. Sci.*, **256**, 2347 (2010).
11. Y. Imal, R. Momoda, Y. Adachi, K. Nishikubo, Y. Kaida, H. Yamada and C.-N. Xu, *J. Electrochem. Soc.*, **154**, J77 (2007).
12. M. Tayebi, S. O. Movahed and A. Ahmadpour, *RSC Adv.*, **9**, 38703 (2019).
13. J. Yan, Z. Tang, S. Luo and Z. Zhang, *Key Eng. Mater.*, **280-283**, 509 (2005).
14. C. Guo, B. Chu and Q. Su, *Appl. Surf. Sci.*, **225**, 198 (2004).
15. X. Lu, M. Zhong, W. Shu, Q. Yu, X. Xiong and R. Wang, *Powder Technol.*, **177**, 83 (2007).
16. H. Wang, X. Liang, K. Liu, Q. Zhou, J. Wang, P. Chen, B. He and J. Li, *Key Eng. Mater.*, **680**, 224 (2016).
17. S. Khursheed, G. A. Sheergojri and J. Sharma, *Mater. Today Proc.*, **21**, 2096 (2020).
18. Q. He and C. Hu, *Opt. Mater.*, **38**, 286 (2014).
19. M. Shi, B. Lu, Y. Jin and M. Ge, *J. Mater. Sci. Mater. Electron.*, **32**, 20804 (2021).
20. Y. Wu, J. Gan and X. Wu, *J. Mater. Res. Technol.*, **13**, 1230 (2021).
21. L. Lyu, Y. Chen, L. Yu, L. Zhang and J. Pei, *Materials*, **13**, 426 (2020).
22. H. L. Frisch, *J. Phys. Chem.*, **61**, 93 (1957).
23. J.-H. Ahn, Y.-S. Jeong, I.-T. Kim, S.-H. Jeon and C.-H. Park, *Sensors*, **19**, 1416 (2019).
24. H. M. Hajar, M. J. Suriani, M. G. M. Sabri, M. J. Ghazali and W. B. W. Nik, *Biosci. Biotechnol. Res. Asia*, **12**, 71 (2015).